



ELSEVIER

January 2003

Materials Letters 57 (2003) 1113–1119

**MATERIALS
LETTERS**

www.elsevier.com/locate/matlet

Graphite with fullerene and filamentous carbon structures formed from iron melt as a lithium-intercalating anode

Y.H. Lee^a, K.C. Pan^a, Y.Y. Lin^b, V. Subramanian^b, T. Prem Kumar^{b,1}, G.T.K. Fey^{b,*}^a*Institute of Materials Research and Engineering, National Taiwan University, 1 Roosevelt Road, Section 4, Taipei 106, Taiwan, ROC*^b*Department of Chemical and Materials Engineering, National Central University, Chung-Li, 32054, Taiwan, ROC*

Received 2 June 2002; accepted 3 June 2002

Abstract

The electrochemical properties of flaky graphite containing carbon nanostructures, synthesized by a dissolution-precipitation method from a carbon-rich cast iron melt, were investigated. The formation of the highly crystalline graphite was realized at temperatures as low as 1600 °C. The presence of fullerenes and filamentous carbon structures on the graphite was confirmed by X-ray diffraction, Raman spectroscopy and scanning electron microscopy. The reversible lithium intercalation capacity of the graphitic product was more than 300 mAh/g. The first-cycle irreversible capacity was a mere 14%. The coulombic efficiency seemed to stabilize at values >99% from the fifth cycle.

© 2002 Elsevier Science B.V. All rights reserved.

Keywords: Dissolution-precipitation; Filamentous carbon; Fullerenes; Nanomaterials; Carbonaceous anode; Lithium-ion batteries

1. Introduction

The elemental chemistry of carbon has undergone a tremendous transformation with the discovery of fullerenes [1] and carbon nanotubes [2]. By virtue of their extraordinary structural, electrical and mechanical properties, these allotropic modifications of carbon hold much promise as microscopic probes [3], single electron transistors [4], nanotweezers [5], hydrogen storage media [6], etc. The production of such nanostructures is laborious and energy-intensive.

Preparation procedures include carbon arc-discharge [2,7,8], laser ablation [9,10] and electron beam irradiation [11]. They may also be prepared by the catalytic decomposition of hydrocarbons on metal catalysts [12–16]. However, the yields from these are very low (about 2%) [17], and the products require careful purification. Thus, there is an immediate need to devise low-cost methods for the preparation of nanocarbon materials. Chernozatonskii et al. [18] reported the synthesis of inclusions of fullerenes and nanotubes in alloys of Fe–Ni–C and Fe–Ni–Co–C at temperatures between 1250 and 1300 °C. Recently, the formation of multi-walled graphite shells wrapped around metallic catalyst particles, cockle-shelled graphite filaments and multi-walled graphite nanotubes was demonstrated by Krivoruchko et al. [19] in the catalytic carbonization of polyvinyl alcohol

* Corresponding author. Tel.: +886-3-422-7151-4206, +886-3-425-7325; fax: +886-3-425-7325.

E-mail address: gfey@cc.ncu.edu.tw (G.T.K. Fey).

¹ On deputation from: Central Electrochemical Research Institute, Karaikudi 630006, TN, India.

over iron particles at 600–800 °C. We have, in a recent communication, shown evidence for the formation of fullerenes in graphites precipitated during the cooling of carbon-rich iron phases [20].

Our interest in these materials is in their applicability as anodes in lithium-ion batteries, for which a low-cost production method is of foremost importance. In this letter, we describe the lithium intercalation–deintercalation behavior of graphite flakes containing nanocarbon structures prepared by a dissolution-precipitation method from a carbon-rich cast iron melt.

2. Experimental

The graphitic material used in this study was prepared by a dissolution-precipitation method in a reducing atmosphere as described elsewhere [20]. Briefly, the method involves the formation of a supersaturated solid solution of amorphous carbon in a melt of cast iron at 1600 °C in a high-frequency induction

furnace and the subsequent precipitation of the carbon as graphite by cooling. The precipitated graphite was recovered by leaching away the metallic constituents with 3 M HCl for 24 h, washing with double distilled water, and drying.

The elemental composition of the graphitic product was determined by a Perkin-Elmer CHN-2000 elemental analyzer. The typical sample weight for elemental analysis was 3 mg. The ICP-AES method (ICP-MS model PE-Sciex Elan 6100DRC) was used for the analysis of residual iron in the graphite. The powder X-ray diffractogram of the graphitic material was recorded on a Philips PW-1710 X-ray diffractometer fitted with a nickel-filtered Cu-K α radiation source between scattering angles of 5° and 80° in steps of 0.05°. Surface morphology was examined by scanning electron microscopy (Hitachi S-4700I). Laser Raman spectroscopic measurements were performed in the 1000–2000 cm⁻¹ region with a laser radiation wavelength of 632.8 nm (Renishaw G-17868 Raman spectrophotometer). The Raman results

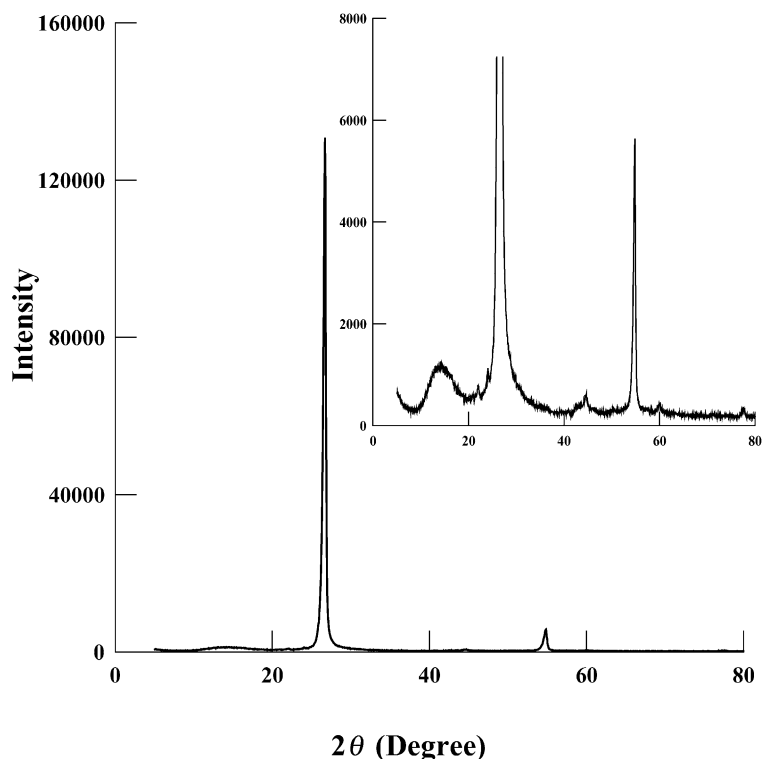


Fig. 1. X-ray diffractogram of the dissolution-precipitated graphite.

were fitted with a Renishaw software. A Rietan software was used for the analysis of the X-ray diffraction data.

The lithium insertion–deinsertion properties of the graphitic material were studied in 2032-type coin cells with a lithium metal foil as the anode and a 1 M solution of LiPF_6 in a 1:1 (v/v) mixture of EC/DEC as the electrolyte. Graphite electrodes for the coin cells were fabricated as follows. The graphitic powder was made into a slurry with 8% PVdF binder and 2% conducting carbon black additive in NMP. The slurry was coated on to a copper foil using the doctor blade method, dried in an oven for 90 min, and roller-pressed. Circular discs were punched out from the coated foil. Cell assembly was done in an argon-filled glove box (VAC Model MO40-1), in which the moisture and oxygen levels were maintained below 2 ppm. Galvanostatic charging and discharging of the cells were done at a 0.1 C rate between 3.0 and 0.05 V in a multi-channel battery tester (Maccor Series-4000).

3. Results and discussion

3.1. Elemental analysis

The percentage composition of the graphitic product was as follows: C (90.17), H (0.55) and N (0.65). The H/C ratio was 0.07. The residual iron content in the product was determined as 9.62 ppm.

3.2. X-ray diffraction

The catalytic effect of iron in the graphitization of carbons in carbon-rich iron melts has been well documented [21–24]. The graphitization process is believed to be due to the G effect [24], a process by which the carbon dissolves in the iron and precipitates out as graphite, or due to the formation and decomposition of carbide intermediates [24]. The sharp XRD peaks indicate that catalytic graphitization occurred at temperatures well below the otherwise high temperatures at which graphitization is normally expected to occur. According to Oberlin and Rouchy [23], heating a non-graphitic carbon with iron results in the formation of a mixture of graphite and a graphitizable phase. The authors [23] believe that an unstable phase of iron carbide is formed, which subsequently decom-

poses to yield iron globules and a shell of graphitizable carbon surrounding the iron.

The powder X-ray diffraction pattern of the graphitic material is shown in Fig. 1. There is a strong peak at a 2θ value of ca. 26° , corresponding to the (002) reflection. This shows that the product was highly crystalline even though the preparation temperature was as low as 1600°C . The reflections for the other hkl indices are comparatively weak, and are shown in the enlarged pattern in the inset. The degree of graphitization was determined to be 92% [20]. Additionally, diffraction peaks could be seen at 2θ values of 13° and 17° , corresponding to reflections of fullerenes. We have already shown by a Rietveld analysis of the XRD data that the graphite contained as much as 4% by weight of fullerene molecules [20].

3.3. Raman spectroscopy

The Raman spectrum of the graphite recorded between 1000 and 2000 cm^{-1} is shown in Fig. 2.

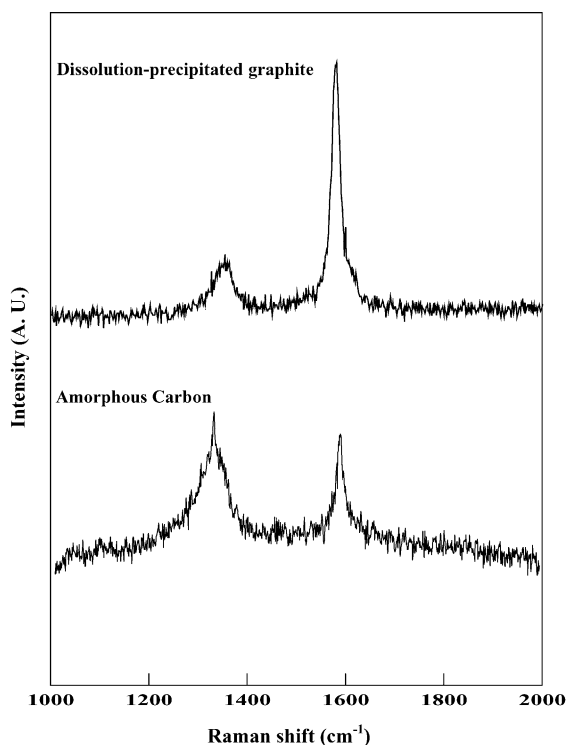


Fig. 2. Raman spectra of the amorphous carbon precursor and the graphitic product.

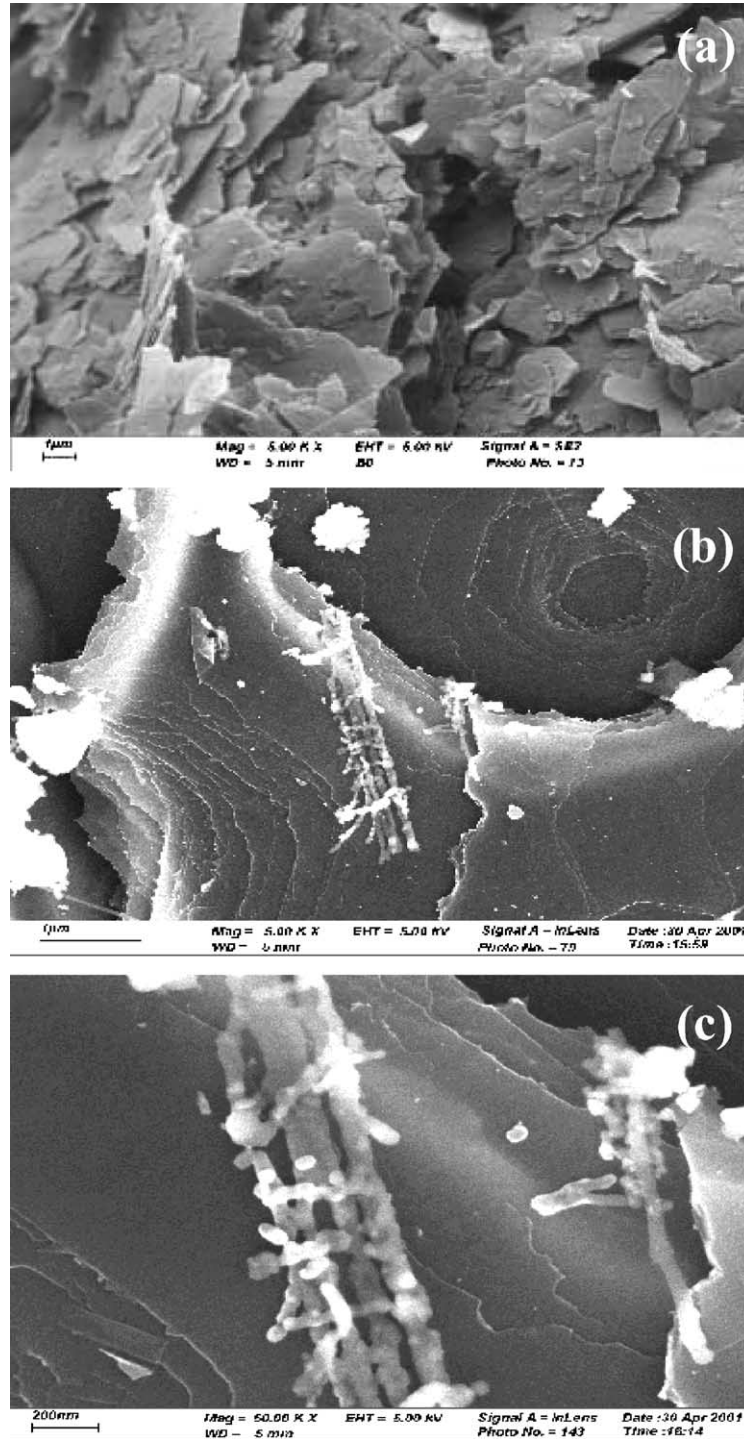


Fig. 3. Scanning electron micrographs of dissolution-precipitated graphite showing (a) a flaky surface morphology; (b) and (c) filamentous and fullerene structures.

For comparison, the Raman spectrum of the amorphous carbon used for the preparation of the graphitic product is also shown. Two bands can be seen in both the spectra, one, the D-band around 1355 cm^{-1} , and the other, the G-band around 1580 cm^{-1} . The G-band is an inherent Raman band for the ideal graphite structure, corresponding to the E_{2g} vibration mode [25]. The D-band, usually identified as the A_{1g} mode, is forbidden for the two-dimensional lattice of graphite according to selection rules. However, for graphite crystallites of finite sizes, the A_{1g} mode will become Raman active [26]. In other words, this band is assigned to defects on the boundary of the carbon layers. It can be seen that the D-band, which appeared as a broad band in the spectrum of the amorphous carbon, became lower in intensity and narrower after graphitization. Similarly, the G-band became sharper, indicating a high degree of graphitization in the product. The ratio of the areas under the two bands (A_G/A_D) registered a sharp increase from 0.3404 for the amorphous carbon to 4.9768 for the graphitic product, indicating a higher degree of graphitization.

3.4. Scanning electron microscopy

Fig. 3a shows the surface morphology of the dissolution-precipitated graphite. Studies have shown that the structural and morphological characteristics of the graphitic materials obtained by the dissolution-precipitation process depend inter alia on the nature of the precursor materials and the thermal history [27]. Our graphite sample had a flaky appearance. Flakiness is a characteristic of dissolution-precipitated graphites obtained from carbon-rich iron melts [25,28]. High-resolution SEM pictures (Fig. 3b and c) show extensive micro-flakiness in the sample. Moreover, fiber-like or filamentous carbon structures with nodular interconnections can also be seen. The bright areas represent high charge density areas, confirming the presence of agglomerations of fullerene structures. The formation of similar structures from hydrocarbons on metal substrates has been reported, although some of the products required high temperatures ($3000\text{ }^\circ\text{C}$) for graphitization [29]. The mechanism of formation of fullerene and tubular structures by rolling or wrapping of an extended planar graphene layer is unclear. However, it appears that such structures are formed by molecular additions in the c direction from hexagonal

graphite precursors. If the carbon atoms are assumed to be interstitial in a matrix of liquid iron [30], molecular assemblies may be expected to result by strong bonding in the a direction as described by the so-called ‘chicken wire’ model [31]. According to Double and Hellawell [30], extensive weak bonding between the hexagonal monolayers in the c direction can lead to flake formation. If a disorderly folding or wrapping occurs, it can lead to spherulitic carbon structures. The formation of fullerene-type molecules, which have a low growth potential, is a specific oriented folding of hexagonal sheets, a process in which a few carbon atoms are eliminated in order to accommodate the carbon pentagons so essential for stereological matching [30].

3.5. Electrochemical studies

It can be seen from Fig. 4 that the dissolution-precipitated graphite gives a high reversible capacity of more than 300 mAh/g over an extended cycling regime. A point to be noted is the low irreversible capacity. The first-cycle irreversible capacity is just 50 mAh/g, a mere 14%. This is much lower than the values commonly reported for irreversible capacities. For example, Chang et al. [32] reported reversible capacities between 217 and 233 mAh/g and irreversible capacities of 25–38% for mesocarbon microbeads graphitized at $2400\text{ }^\circ\text{C}$. The corresponding values for mesocarbon microbeads graphitized at $3000\text{ }^\circ\text{C}$ were 282–299 mAh/g and 21–30%. Thus, the present material combines the twin advantage of a high reversible capacity and a low irreversible capacity. Furthermore, the cyclability of the material improves with

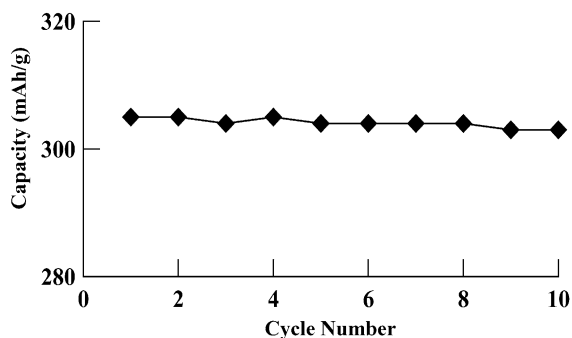


Fig. 4. A typical cycling behavior of a coin cell with the dissolution-precipitated graphite.

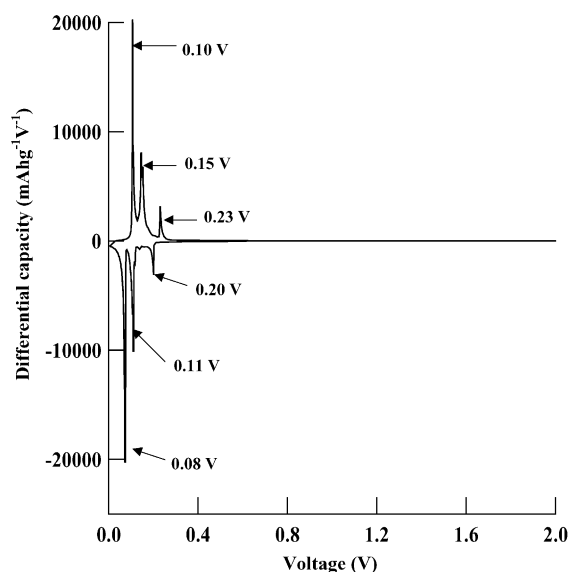


Fig. 5. Differential capacity plot for the lithium intercalation/deintercalation processes in dissolution-precipitated graphite.

cycle number. The coulombic efficiency gradually rises from 98.0% in the second cycle to 99.0% in the fifth cycle and to 99.3% in the tenth cycle. A differential capacity plot derived from the data for the second charge–discharge cycle is given in Fig. 5. The different stages of intercalation can be discerned from the plot. The clear demarcation of the various stages is a hallmark of highly graphitized structures. As can be seen from the figure, there are three well-defined peak potentials during lithium insertion (charging of graphite) at 0.20, 0.11 and 0.08 V. The peaks corresponding to the deinsertion processes appear at 0.10, 0.15 and 0.23 V. Thus, it is clear that all the electrochemical processes that contribute to capacity occurred below 0.25 V. Two interesting things about this material synthesized by the dissolution-precipitation method are the high capacity and cycling efficiency. The high capacities may be related to the high degree of graphitization as well as to the additional sites provided by the carbon nanostructures on the graphites. Fullerenes [33–35] and carbon nanotubes [36–38] have been demonstrated to yield lithium insertion capacities of as much as 1400 mAh/g. Although the content of such nanostructured materials in the graphite is only 4%, it is believed that they too contribute to the lithium intercalation capacity.

Further work is required to quantify the contribution of nanotubular carbon structures to the capacity of the graphites under study here. Most significantly, we have demonstrated that the dissolution of carbon into iron melts and its subsequent precipitation can offer a relatively convenient and low-energy process for the synthesis of nanostructured carbon materials with high lithium intercalation capacities.

4. Conclusions

Electrochemical lithium insertion properties of a crystalline graphitic material derived by the catalytic graphitization (dissolution-precipitation) method in melts of cast iron were studied. The formation of the highly crystalline graphite was realized at temperatures as low as 1600 °C. The presence of fullerenes and filamentous carbon structures on the graphite was confirmed by X-ray diffraction, Raman spectroscopy and scanning electron microscopy. The graphitic product could reversibly intercalate more than 300 mAh/g equivalent of lithium. The first-cycle irreversible capacity was a mere 14%. The coulombic efficiency seemed to stabilize at values >99% from the fifth cycle.

Acknowledgements

This work was carried out under contract no. NSC-90-2214-E-008-051 of the National Science Council of the Republic of China. VS and TPK thank the NSC for the award of post-doctoral fellowships.

References

- [1] H. Kroto, J. Heath, S. O'Brien, R. Curl, R.E. Smalley, *Nature* 318 (1985) 162.
- [2] S. Iijima, *Nature* 354 (1991) 56.
- [3] H. Dai, J.H. Hafner, A.G. Rinzler, D.T. Colbert, R.E. Smalley, *Nature* 384 (1996) 147.
- [4] M. Bockrath, D.H. Cobden, P.L. McEuen, N.G. Chopra, A. Zettl, A. Thess, R.E. Smalley, *Science* 275 (1997) 1922.
- [5] P. Kim, C.M. Lieber, *Science* 286 (1999) 2148.
- [6] A.C. Dillon, K.M. Jones, T.A. Bekkedahl, C.H. Kiang, D.S. Bethune, M.J. Heben, *Nature* 386 (1997) 377.
- [7] T.W. Ebberson, P.M. Ajayan, *Nature* 358 (1992) 220.
- [8] H.J. Muhr, R. Nesper, B. Schunger, R. Kotz, *Chem. Phys. Lett.* 249 (1996) 399.

- [9] T. Guo, C. Jin, R.E. Smalley, *J. Phys. Chem.* 95 (1991) 4848.
- [10] A. Thess, R. Lee, P. Nikolaev, H. Dai, P. Petit, J. Robert, C. Xu, Y.H. Lee, S.G. Kim, A.G. Rinzler, D.T. Colbert, G.E. Tomanek, J.E. Fischer, R.E. Smalley, *Science* 273 (1996) 483.
- [11] T. Fuller, F. Banhart, *Chem. Phys. Lett.* 254 (1996) 372.
- [12] M. Endo, *Chemtech* (1988) 568.
- [13] V. Ivanov, A. Fonseca, J.B. Nagy, *Carbon* 33 (1995) 1727.
- [14] T. Kyotani, L.F. Tsai, A. Tomita, *Chem. Mater.* 7 (1995) 1427.
- [15] H. Dai, A.G. Rinzler, P. Nikolaev, A. Thess, D.T. Colbert, R.E. Smalley, *Chem. Phys. Lett.* 260 (1996) 471.
- [16] M. Terrones, N. Grobert, J. Olivares, J.P. Zhang, H. Terrones, K. Kordatos, W.K. Hsu, J.P. Hare, P.D. Townsend, K. Prasad, A.K. Cheetham, H.W. Kroto, D.R.M. Walton, *Nature* 388 (1997) 52.
- [17] K. Tohji, T. Goto, H. Takahashi, *Nature* 383 (1996) 679.
- [18] L.A. Chernozatonskii, V.P. Val'chuk, N.A. Kiselev, O.I. Lebedev, A.B. Ormont, D.N. Zakharov, *Carbon* 35 (1997) 749.
- [19] O.P. Krivoruchko, N.I. Maksimova, V.I. Zaikovskii, A.N. Salanov, *Carbon* 38 (2000) 1075.
- [20] Y.H. Lee, Y.C. Chang, K.C. Pan, S.T. Chang, *Mater. Chem. Phys.* 72 (2001) 232.
- [21] S.B. Austerman, S.M. Myron, J.W. Wagner, *Carbon* 5 (1967) 549.
- [22] Y. Hishiyama, A. Ono, T. Tsuzuku, *Carbon* 6 (1968) 203.
- [23] A. Oberlin, J.P. Rouchy, *Carbon* 9 (1971) 39.
- [24] A. Oya, S. Otani, *Carbon* 19 (1981) 391.
- [25] S. Liu, C.R. Loper, *Carbon* 29 (1991) 1119.
- [26] M. Audier, M. Oberlin, A. Oberlin, M. Coulon, L. Bonnetain, *Carbon* 19 (1981) 217.
- [27] W. Wang, K.M. Thomas, R.M. Poultney, R.R. Willmers, *Carbon* 33 (1995) 1525.
- [28] S. Liu, C.R. Loper, *Carbon* 29 (1991) 547.
- [29] N.M. Rodriguez, *J. Mater. Res.* 8 (1993) 3233.
- [30] D.D. Double, A. Hellawell, *Acta Metall. Mater.* 43 (1995) 2435.
- [31] D. Ugarte, *Chem. Phys. Lett.* 207 (1993) 473.
- [32] Y.C. Chang, H.J. Sohn, C.H. Ku, Y.G. Wang, Y. Korai, I. Mochida, *Carbon* 37 (1999) 1285.
- [33] Y. Chabre, D. Djurudo, M. Armand, W.R. Romanow, N. Coastel, J.P. McCauley Jr., J.E. Ftsehes, A.B. Smith III, *J. Am. Chem. Soc.* 114 (1992) 7649.
- [34] S. Lemont, J. Ghanbaja, D. Billaud, *Mol. Cryst. Liq. Cryst.* 244 (1994) 203.
- [35] L. Firlej, A. Zahab, F. Brocard, P. Bernier, *Synth. Met.* 70 (1995) 1373.
- [36] J.C. Withers, R.O. Loutfy, J.P. Lowe, *Fuller. Sci. Technol.* 5 (1997) 1.
- [37] V.A. Nalimova, D.F. Skovsky, G.N. Bondarenko, H.A. Gaucher, G. Bonamy, F. Beguin, *Synth. Met.* 88 (1997) 89.
- [38] G.T. Wu, C.S. Wang, X.B. Zhang, H.S. Yang, Z.F. Qi, P.M. He, W.Z. Li, *J. Electrochem. Soc.* 146 (1999) 1698.